IEEE Access
Multidisciplinary | Rapid Review | Open Access Journal

Received June 20, 2020, accepted July 8, 2020, date of publication July 15, 2020, date of current version July 27, 2020.

Digital Object Identifier 10.1109/ACCESS.2020.3009531

Design and Characterization of T/R Module for Commercial Beamforming Applications

MOH CHUAN TAN[1,2], (Graduate Student Member, IEEE), MINGHUI LI[1], (Member, IEEE), QAMMER H. ABBASI[1], (Senior Member, IEEE), AND MUHAMMAD ALI IMRAN[1], (Senior Member, IEEE)

[1]James Watt School of Engineering, University of Glasgow, Glasgow G12 8QQ, U.K.
[2]Research and Development Department, RFNet Technologies Pte Ltd., Singapore 319319

Corresponding author: Moh Chuan Tan (tmohchuan@rfnetech.com)

This work was supported in part by the Engineering and Physical Sciences Research Council (EPSRC) Global Challenges Research Fund, Distributed Autonomous and Resilient Emergency Management System (DARE) Project under Grant EP/P028764/1.

ABSTRACT In the smart antenna system, the transmit and receive (T/R) module is one of the core components as it accounts for nearly 45% of the overall smart antenna system cost. Due to the high implementation cost of the T/R module, the literature was mainly centered around the military and satellite radar applications. However, over the years, the cost of the T/R module has been reduced drastically by leveraging on the advanced manufacturing technology, volume production pricing and adaptation of the commercially available off-the-shelf components, as a result, the adoption of the T/R module in commercial and industrial application become possible. In this work, we have proposed a commercially affordable T/R module that operates in 4.9–5.9 GHz band for commercial and industrial applications. The T/R module was designed, calibrated, and characterized for use in the beamforming smart antenna system. The design process including the circuit, schematic and printed circuit board (PCB) were highlighted. The proposed recursive calibration process managed to correct the phase error to $\pm$ 1° and amplitude error to $\pm$ 0.2 dB. In addition, the amplitude distribution of 0.5-1-1-0.5 combination has successfully suppressed the side-lobe level (SLL) to $-$28.7 dB for 0°, $-$22.71 dB for $\pm$ 20° and $-$12.77 dB for $\pm$ 40° beam steering. This work is aimed to promote the adoption of the T/R module into the commercial and industrial applications such as public or government infrastructure.

INDEX TERMS T/R module, smart antenna, amplitude distribution, beamforming, commercial applications.

I. INTRODUCTION

In the smart antenna industry, the hybrid beamforming (HBF) technique is one of the techniques that attracted many researchers due to its simplicity, cost-effectiveness and being able to achieve comparable results as compared to the digital beamforming. HBF combines both analog and digital beamforming components that are able to perform beamforming digitally and maintain the low cost. The HBF architecture consists of a low-dimensional digital beamformer and a radio frequency (RF) beamformer implemented using the phase shifters, targeted to achieve low deployment cost and high scalability. The advantages of the HBF system has been reported in [1] applications in Large scale antenna systems (LSAS), [2] wireless power transfer (WPT) and [3] antenna system with limited space and power.

RF beamforming frontend is one of the most important components in the HBF system. The RF beamforming frontend has been evolved over the years, and the subsystem has been modularized and miniaturized using the commercially off-the-shelf (COTS) components into the transmit and receive (T/R) module that increases the deployment friendliness and the cost benefits by mass-producing the T/R modules. In [4], the authors pointed out the importance of the T/R module that can be integrated as the slat and tile architecture for the Multifunction Phased Array Radar (MPAR), significant cost reduction of the T/R module was contributed by the increases in production volume and the advancement in automated assembly and test equipment. In [5], the authors highlighted that in the military phased array radar systems, detailed cost figures of the main segments are indicating that

The associate editor coordinating the review of this manuscript and approving it for publication was Raghvendra Kumar Kumar Chaudhary.

the T/R module of the phased array antenna accounts for nearly 45% of the system cost and justify the cost of the T/R module is crucial to determine the total system cost. In [6], the Arrays at Commercial Timescales (ACT) program constitutes a forward-looking approach to the design, construction, and upkeep of phased arrays accomplished through modular array component architectures T/R modules that leverage on commercial semiconductor technologies that evolve at much faster rates than traditional RF components.

Due to the high implementation cost, the early adoption of the T/R modules was mainly focused on military applications. The advancement in the manufacturing technology and commercially available radio frequency integrated circuits (RFIC) or chipset had further reduced the cost of the T/R module and contributes to the higher demand of such modules, the application of the T/R module has gained its momentum and broadened its coverage into other frequency bands. For instance, an L and C-band T/R module for active phased array radar applications has been reported in [7], in [8] and [15] where various types of transceiver modules operate between X, W and Ka-band have been proposed using the silicon-germanium (SiGe) technology. In [9], the S-band T/R module was developed using gallium arsenide (GaAs) monolithic microwave integrated circuit (MMIC). In [10] the T/R module was developed into the C-Band using the multi-chip module (MCM). In X-band, [11], [12] and [13], the T/R module were developed using gallium nitride (GaN) MMIC, liquid cooling micro-channels structure integrated into low-temperature co-fired ceramic (LTCC) substrate and complementary metal-oxide-semiconductor (CMOS) RF system on a chip (SoC) with GaAs RF frontend IC respectively. In [14], the LTCC was used to design the T/R module.

Performance parameters characterizations are the key tasks that require much attention during the design of the T/R module. In the beamforming process [19], both the amplitude and phase of each antenna element are controlled. A combined amplitude and phase control or ''complex weight'' can be used to adjust the side-lobe level (SLL) and steer nulls more accurately as compared to the improvement by phase control alone. Therefore, the precision of the amplitude and the phase of the RF beamforming frontend is extremely important to ensure the accuracy of the beam steering. The RF beamformer frontend shall be properly characterized and calibrated to offset the phase and amplitude error that were contributed by i) manufacturing tolerance such as printed circuit board (PCB) materials and process variations, ii) components tolerances, iii) performance variations due to frequency response and thermal effect, etc.

Amplitude calibration involves calibrating the transmit output power of the T/R module over the operating frequency, the value is utilized to set the amplitude distribution from the T/R module to each antenna port during beamforming process. Some well-known amplitude distribution techniques are listed here, (i) Uniform distribution, where the amplitudes at all the antenna ports are set equal, and the best gain and-half power beamwidth (HPBW) can be achieved while the SLL suffered, (ii) Optimum distribution with the amplitudes being highest at the middle ports and gradually decreasing towards the side of the other ports, this technique produces the moderate gain, HPBW and SLL performance, while (iii) Binomial distribution provides the best SLL performance but suffers from lower gain and wider HPBW. In [16], the authors revealed that the Tschebyscheff distribution delivers the best SLL compared with the uniform and binomial amplitude distributions of the linear patch antenna array. In [17], the authors demonstrated that the grating lobes appear if the amplitude distribution within a module and a system of modules are independent of each other. In [18], the amplitude taper function was applied to improve the SLL of the phased array antenna system, and approximately 10 dB improvement on the SLL level was demonstrated.

Phase calibration is required to correct the inherited phase error of the T/R module due to manufacturing tolerances. In [20], a phase optimization procedure based on the local search and the simulated annealing (SA) algorithm has been proposed to achieve more accurate beamforming of the phased array. A simple calibration procedure has been proposed in [21] to decrease the phase deviation during phase shift and gain control, the calibration results show that the phase error has been drastically mitigated.

In this work, we are focusing on the highly scalable T/R module that was designed to support commercial band in 4.9–5.9 GHz for linear phased array [22] applications in an HBF antenna system. The T/R module was designed using the commercially available off-the-shelf components using GaAs MMIC that is flexible to be integrated into the conventional phased array to form a smart beamforming antenna system. A simple iteration-based method is proposed to calibrate the amplitude and phase error of the T/R Module. The amplitude distribution of the beamforming system has been simulated and the results were experimentally validated. A customized T/R module has been developed instead of the off-the-shelf RF frontend which has limited control features that are important to realize the accuracy of the beamforming function, such as the wide dynamic gain control, high-resolution phase control, fast RF switching to support up to 4 antennas with the single chain and gain boost for transmitter and receiver.

The rest of this paper is organized as follows. Section II presents the design approach for the T/R module, including the hardware architecture, schematic and PCB design, the prototype of the T/R module that has been fabricated. In section III, the phase, transmit power and amplitude distributions are characterized using the simple recursive calibration method. Section IV demonstrates the beamforming performance of the T/R module in the antenna system; the accuracy of the beam steering angle and side-lobe improvement has been validated. Section V concludes the paper.

II. T/R MODULE DESIGN

The block diagram of the T/R module is presented in Fig. 1. The T/R module has both transmitter and receiver functions

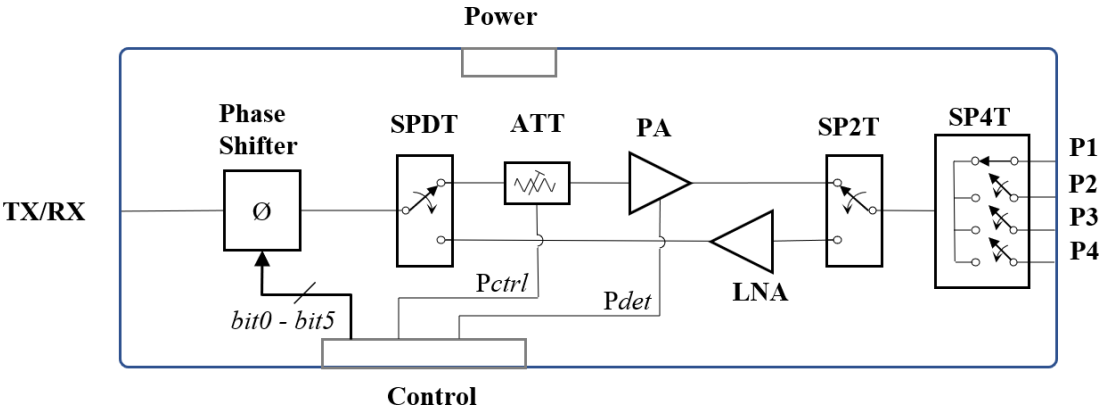

FIGURE 1. Block diagram of the RF chain for n × 4 array.

that can be switched using the single pole two throw (SP2T) switch. Each T/R module consists of necessary components such as the power amplifier (PA), low noise amplifier (LNA), phase shifter, attenuator, RF switched and control peripherals to support the necessary functions required to steer the radiating beam of the phased array. The T/R module was designed to operate from 4.9–5.9 GHz. Each T/R module is designed to support an n × 4 antenna array with the built-in high-speed single pole four throw (SP4T) RF switch to switch between the element in the n × 4 array. Each n × 4 array is capable of performing 90° sector scanning, and only 4 sets of T/R modules are needed to support 4 units of n × 4 arrays to form a 360° beamforming antenna system. The T/R module was designed using COTS components and commercial manufacturing technology, that increases its scalability and further cost reduction by volume production, the recursive calibration was introduced to enhance the T/R module performance and necessary calibration during the mass production. The circuits design consideration of the T/R module is explained below.

Receiver, the main function of the receiver is to amplify the RF signal received from the antenna and to keep the noise figure as low as possible to achieve the good receiver sensitivity, hence the LNA has to be placed as close as possible to the antenna. The receiver power budget is calculated as follow, the attenuation of the phase shifter is 5 dB, SP2Ts are 2.6 dB, SP4T is 1.7dB, PCB and connector loses is 3 dB, with the input power of −90 dBm and the LNA gain of 14.5 dB, the calculated receiver output is −87 dBm, which is sufficient to compensate for the attenuation due to components. The attenuation factor of the individual COTS components is carefully selected to meet the power budget requirement. The phase shifter is placed at a common path where it can be shared between the transmitter and receiver via an SP2T switch, the 6-bits digital phase shifter with 5.625° resolution can be adjusted digitally via bit0 - bit5 to control the phase of the received signal during the beamforming operation.

The beam steering direction, θ can be varied by setting the phase shift, $\Delta\emptyset$ of the two successive elements [23] as shown in Fig. 2 and it can be represented by equation (1) to (3).

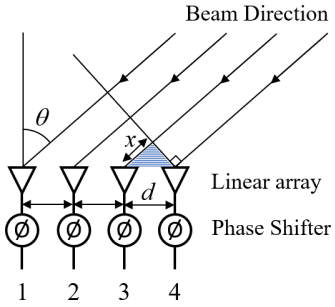

FIGURE 2. Phase shifter in a beamforming linear array.

A shaded right-angle triangle can be drawn between the radiator plane and the beam direction that gives,

$$x = d \cdot sin\theta \tag{1}$$

The distance x can be expressed with respect to the wavelength,

$$\frac{\lambda}{x} = \frac{360^\circ}{\Delta\emptyset} \tag{2}$$

where x is the shorter side of the triangle that lies on the beam, d is the separation of the elements, θ is the direction of the beam steering, the array boresight is defined as 0°, λ is the wavelength and $\Delta\emptyset$ is the phase difference between two successive elements. Substitute equation (1) into (2) gives,

$$\Delta\emptyset = \frac{360^\circ \cdot d \cdot sin\theta}{\lambda} \tag{3}$$

A 5.5 GHz linear array with 27.25 mm elements separation, and the phase shift, $\Delta\emptyset$ of 45° between the successive elements will produce a beam steering direction of 14.5°. The beam steering resolution is determined by the resolution of the phase shifter, a 6-bit phase shifter with 5.625° lowest bit resolution will give approximately 2° beam steering resolution.

Transmitter, the transmitter function is to boost the RF signal before it is transmitted to the air via the antenna, the PA is included to boost the RF signal and compensate the insertion loss exhibited by the phase shifter, RF switches

and insertion loss due to PCB traces, where the internally matched 3-stages commercially available PA was used to minimise the antenna mismatch and possibly degrade the transmitter performance during the beamforming operation. An RF attenuator was included before the PA to attenuate the RF power before entering the PA, it provides a 30 dB dynamic transmit power range. Similar to the receiver, the phase of the transmitted signal can be adjusted by controlling a digital phase shifter located at the common path. The amplitude and phase are necessary to vary in order to set the weight of the RF signal that is required during the beamforming process. The transmitter power budget is calculated as follow, the attenuation of the phase shifter is 5 dB, SP2Ts are 2.6 dB, SP4T is 1.7dB, PCB and connector loses is 3 dB, with the target input power of 5 dBm, PA gain of 30 dB and attenuator range of 0 - 30 dB, the targeted output power calculated around -7.3 to 22.7 dBm with approximately 30 dB dynamic range. Similarly, the attenuation factor of the individual COTS components is carefully selected to meet the power budget requirement.

RF Switches, two types of RF switches are used in the T/R module design, i) SP2T, to switch between the transmitter and receiver path and provides 51 dB isolation between the transmit and receive ports to minimise the self-excitation due to the signal feedback during transmit and receive operations. The HMC8038LP4CETR is widely used in Wireless Lan applications to switch between the transmitter and receiver path, and it has a switching timing of 150 ns which is sufficient to support the half-duplex transceiver that has more than 150 ns wait time between the transmit and receive operations, for instance, 802.11 wireless LAN with the short interframe space (SIFS) duration of 10 μs, the SIFS is the time from the end of the last symbol of the previous frame to the beginning of the first symbol of the preamble of the subsequent frame. In 802.11 WLAN, one SIFS duration elapses, the transmission can immediately start, ii) SP4T, is a high-speed RF switch to switch between each element in the phased array for the beam scanning operation [24] to channel the RF signals to the high-speed processor or FPGA for decoding. The SP4T has a switching time of around 19 ns, the estimated symbol processing time for the FPGA and processor can be computed by taking the symbol duration divided by 4 minuses away the switching time, for instance, the symbol duration for 802.11n WLAN is 6.8 μs, this will allow the processor to has 1.681 μs to process the symbol received from each antenna element, thus the direction of arrival can be determined. In addition, to avoid the port mismatch that causes the signal reflected from the antenna ports, PA and LNA, the ports at the RF switches are made non-reflective with 50-ohm termination design when the port is not active.

Power Supply, The T/R module is powered by the multiple power supplies $+5$V, $+3.3$V, -3.3V and -5V, any stable commercially available power source can be used to power up the T/R module. When multiple T/R modules are cascaded for bigger beamforming system, a common power supply can be used to power up all the T/R modules in the cascaded system.

Electrical Interface and Control, now the design and the specifications of the T/R module are specified, next step is to define the various control methodology and steps required to evaluate the T/R module and automatic adjustment on various RF parameters when the T/R modules are placed into the beamforming antenna systems. The power and control of the T/R module are connected to the external power supply and the interface controller via the 6-way and 14-way cable assembly from Molex, PicoBlade series. The interface controller board was designed such that it allows manual control via dip switches for digital control and resistive trimmer for analog control signal, for instance as shown in Fig. 1, bit0 to bit5 transistor-transistor logic (TTL) for phase adjustment, analog voltage signal P*ctrl* to control the transmit power of the RF chain and the analog signal P*det* that can be used to monitor the transmit power generated by the PA. The T/R module was designed with 4 mounting holes to allow stack-up arrangement using brass stand-off. The picture of the 4 T/R modules in a stack-up arrangement is shown in Fig. 3.

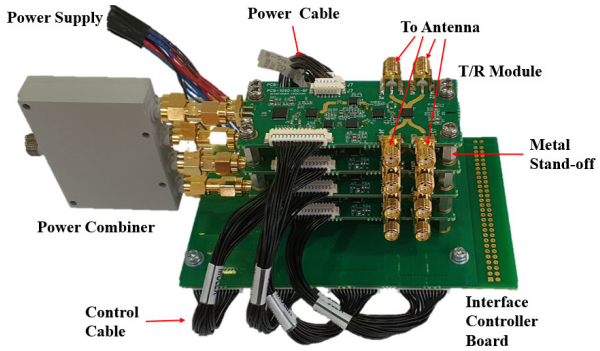

FIGURE 3. T/R modules mounted on the interface controller board.

The T/R module is designed using the commercially available components mounted on a commercially low-cost PCB. The key components used in the T/R module and their key specifications are listed in TABLE 1 below.

A. SCHEMATIC AND PCB DESIGN

The Schematic capture and PCB layout are designed using Power Logic and Power PCB from Mentor Graphic [25]. The T/R module is a 4-layers PCB board, each layer of copper is 0.7mil thickness and separated by the dielectric substrates. The top layer substrate is R04003 materials with 8 mils thickness for optimum RF performance, and the middle and bottom layers substrate are the lower cost FR-4 material. The total PCB thickness is 62 mils. The price of the PCB material fluctuates based on the market demand and supply, the general guideline of the cost factor ratio between the FR4 and RO4003 is 1:5, therefore it's justifiable to use RO4003 only for the critical layer and replace the rest of the layers with the low-cost FR4 material.

The RF traces and the signal line are routed at the top layer, the second layer provides a solid ground plane for good RF performance, third and fourth layers provide additional

TABLE 1. Key components specifications.

Parts	Part Number/ Maker	Key Specifications
Phase Shifter	HMC1133LP5E/ ADI	Phase Resolution: 5.625° Phase Coverage: 360°
RF Attenuator	IDTF2258NLGK/ IDT	Insertion Loss: 2.7 dB Attenuation Range: 33.6 dB
Power Amplifier	TQP5525/ Qorvo	Gain; 32 dB P1dB: 32 dBm
LNA	HMC717ALP3E/ ADI	Noise Figure: 1.3 dB Gain: 14.5 dB P1dB: 18 dBm
RF Switch (SP2T)	HMC8038LP4CE TR/ ADI	Insertion loss: 1.3dB Ports Isolation: 51 dB
RF Switch (SP4T)	ADRF5044/ ADI	Insertion Loss: 1.7 dB Switching Speed: 19 ns Ports Isolation: 55 dB

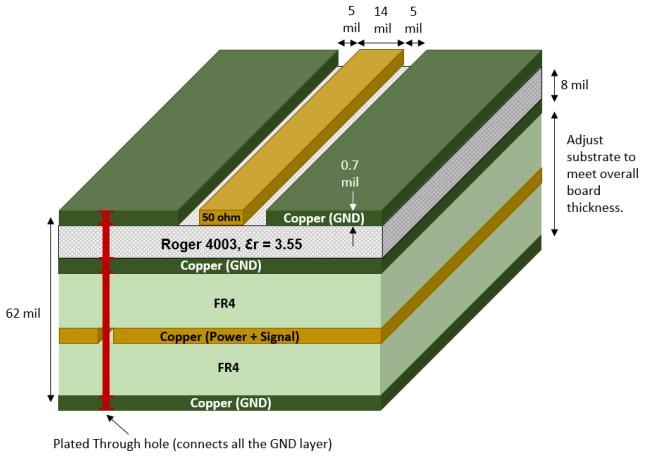

FIGURE 4. The PCB cross-sectional view of the T/R module.

ground and power supply routing. All the components are mounted at the top layer to ease the assembly process and troubleshooting. The stacked-up construction of the PCB is shown in Fig. 4.

The transmission line is constructed using the coplanar waveguide (CPWG) model, where the characteristic impedance of the 14 mils traces with 5 mils ground plane spacing is 50-ohm. Substrate RO4003 with dielectric constant $\varepsilon r = 3.55$ and 8 mils thickness is sandwiched between the impedance-controlled traces and the ground plane, and the thickness of the 2 layers of FR4 substrate will be adjusted to meet the total board thickness of 62 mils.

The PCB layout was designed with the following consideration, i) impedance control, all the RF traces are laid on the top layer for better CPWG impedance control with a solid copper plane on the second layer separated by RO4003 substrate, and the impedance controlled traces are highlighted in orange as shown in Fig. 5, ii) Electro Magnetic Compatibility (EMC) consideration, the control signals, power plane and additional ground plane are laid on layer 3, layer 4 consists of

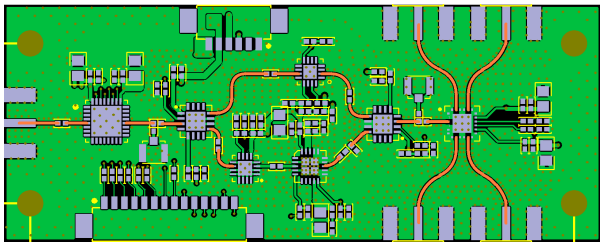

FIGURE 5. Impedance controlled traces (orange traces).

a solid ground plane that acts as a shield for optimum EMC performance, iii) thermal consideration, the heat-generating components such as PA will have its metal body soldered directly to the big copper plane on the top later of the PCB, and the bottom layer of the PCB will have an exposed copper to install the heatsink when needed, iv) cost consideration, the RO4003 substrate material cost is relatively higher compared to FR-4 material, therefore except the substrate between layer 1 and layer 2 is utilizing RO4003, FR-4 substrate will be used for all other layers where the impedance control is not required. The PCB layout layers stack-up is shown in Fig. 6.

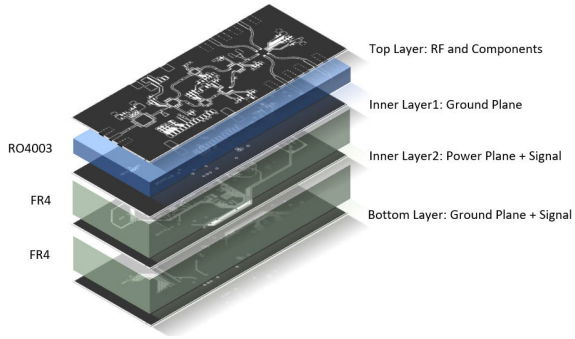

FIGURE 6. PCB layers stack-up of the T/R module.

The T/R module is assembled with components using Surface Mount Technology (SMT), the solder paste is deposited onto the PCB solder pads using the stencil mask, components are placed onto the PCB using SMT machine for tape and reel part or manually for loose components, after which the board is passing through a reflow oven to solidify the solder thus holding the components in solid solder joint. The top view of the beamformer boards after assembly is shown in Fig. 7.

B. THE PROTOTYPE OF THE T/R MODULE

The prototype of the T/R module is presented in Fig. 7. The P1–P4 and TX/RX ports can be easily connected to external RF equipment via the Sub-Miniature version A (SMA) connectors, the power supply and control of the T/R module are connected to the external power supply and the interface controller or test fixture to allow external control during the performance evaluations.

A Test fixture has been developed to aid the evaluation of the T/R module, and the prototype of the test fixture is shown

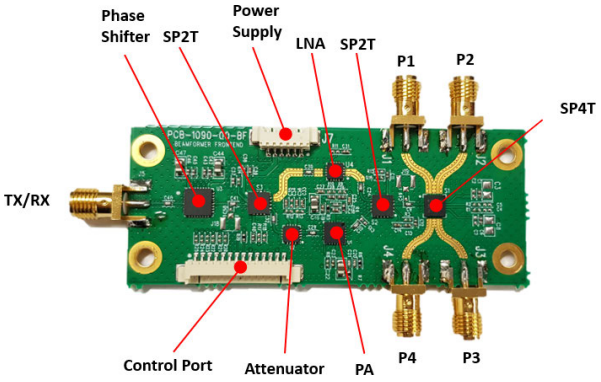

FIGURE 7. The prototype of the T/R module.

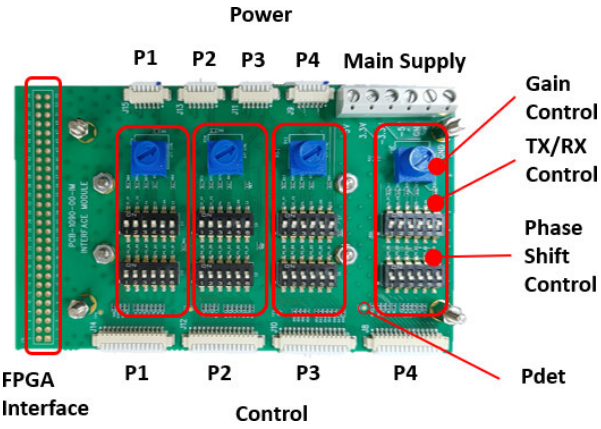

FIGURE 8. The prototype of the test fixture.

in Fig. 8. The building block of the test fixture consists of the dip switches to digitally control the RF components of the T/R module such as SP2T, SP4T, phase shifter and turning on and off the PA and LNA, an analog control by the resistive trimmer to tune the analog voltage that is required to adjust the attenuation of the attenuator, analog voltage monitoring to monitor the voltage level of the power detector output which is used to determine the actual transmitted power. In addition, the common power supplies provide the power sources and distribute them to the multiple T/R modules when they are cascaded. Provision has been provided by pulling out all the signals to a header, that can be connected to a microcontroller of FPGA for automated control during testing and beamforming operation.

III. RF PARAMETER CHARACTERIZATION

The RF parameters such as transmit power or amplitude and phase errors are characterized using the recursive calibration approach, and the calibrated parameters are stored in the memory and will be used for self-compensation during the beamforming process. The SLL of the beam can be optimized by varying the amplitude of each antenna ports which is represented by amplitude distribution. The calibration setup of the T/R module is shown in Fig. 9, the phase shifter is controlled by the 6 bits TTL signal, the output power is controlled by

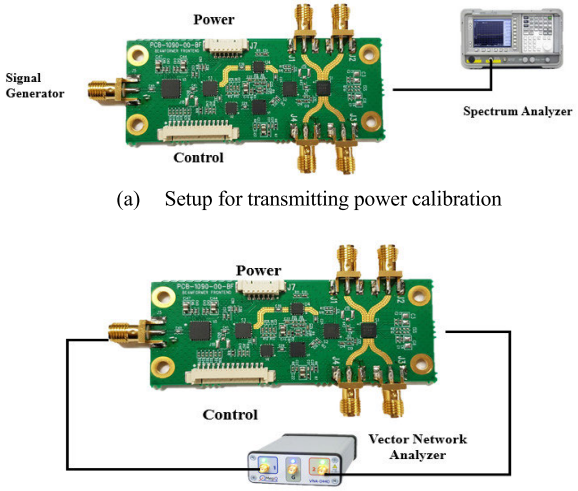

FIGURE 9. Calibration setup.

adjusting the RF attenuator via the analog control signal P*ctrl* through an external power source, and the output power level is detected and converted to an analog voltage, P*det* that will be used to monitor the output power level during the calibration. A Spectrum Analyzer (SA) and a Vector Network Analyzer (VNA) are used to measure the transmit power and phase shift of the T/R module. The equipment is connected to the individual port namely P1 to P4 to perform the calibration on the respective port.

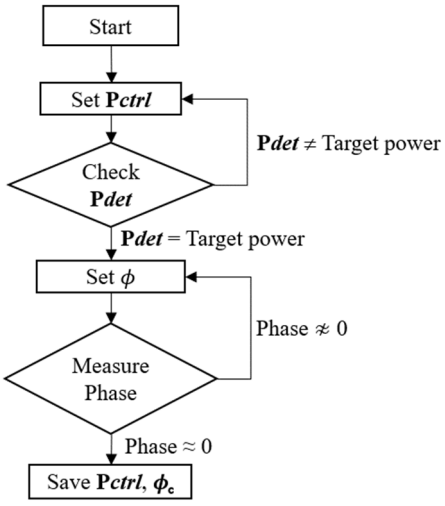

FIGURE 10. Iteration flow for power and phase calibration.

The transmit power response will be first characterized using the spectrum analyzer as shown in Fig. 9a, followed by the phase offset calibration using VNA as shown in Fig. 9b. The iteration flow involved in the calibration of the transmit power and phase is illustrated in Fig. 10. During the power detector P*det* calibration, the P*ctrl* voltage is adjusted between 0 V and 3 V, and the output power of the T/R module and P*det* voltage is constantly measured, thus the relationship between P*ctrl*, P*det* and the output power can be plotted, refer

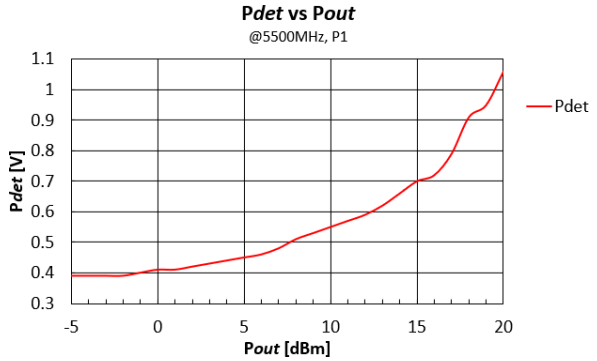

FIGURE 11. Output power and P*det*.

to Fig. 11. Once the P*det* characterization is done, the phase calibration can be carried out by controlling the P*ctrl* and monitoring the P*det* for constant power calibration, the phase error is observed by the VNA and iterated by controlling bit0 to bit5 of the phase shifter. The calibration process continues for other variables such as the frequency, and power, and repeats for Port 2, 3 and 4.

A. CHARACTERIZING THE RF OUTPUT POWER

The power control of the RF chain is achieved by controlling the attenuator. The attenuation performance of the RF chain is shown in Fig. 12, the control voltage, Pctrl is ranged from 0.7 to 2.0 V, where 0.7 V gives 0 dB attenuation and the maximum attenuation of 30 dB occurs at 2.0 V.

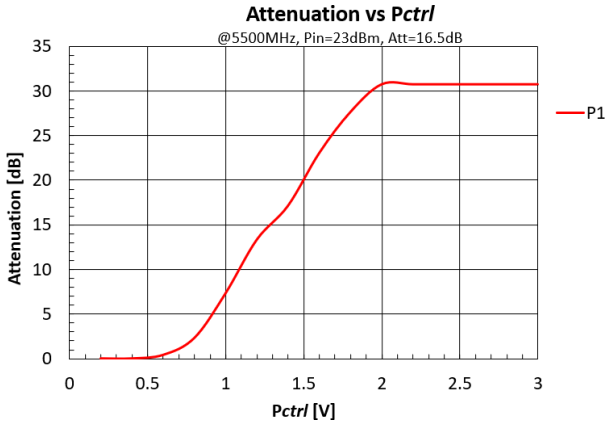

FIGURE 12. Power attenuation performance.

In most of the cases, the output power of the RF chain varies according to the frequency and thermal response. The RF calibration will help to define the appropriate P*ctrl* to produce a flat transmit power response over the intended operating condition. The frequency response chart for the transmit power is shown in Fig. 13, with P*ctrl* being at 0.8 V, the transmit output power tolerance as shown in the blue line is around +/2 dB over the frequency range from 5180 to 5880 MHz. The variation is probably due to the components and PCB manufacturing tolerances. The red line represents the transmit power after power calibration, the tolerance is improved to +/− 0.2 dB. The P*ctrl* voltage set

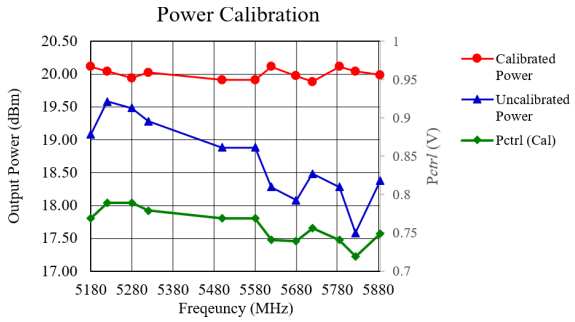

FIGURE 13. Output power calibration.

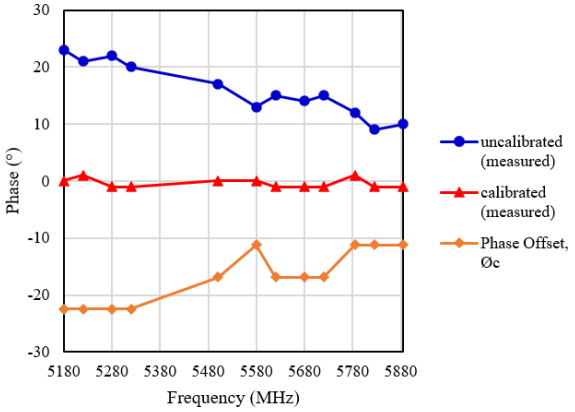

FIGURE 14. Phase calibration.

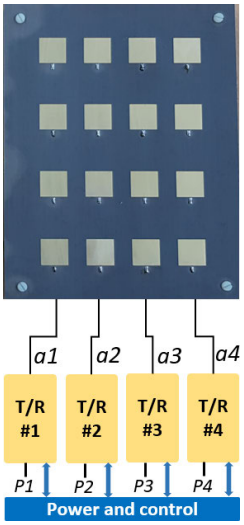

FIGURE 15. Gain distribution model on the 4 × 4 array.

to calibrate the transmit power is represented by the green line.

The gain flatness can be compensated automatically by initial calibration or calibration on-the-fly where the P*det* can be monitored regularly and the output power can be adjusted using the P*ctrl*, and the automated adjustment procedure will make sure each of the RF chains to transmit at its desired power. The maximum measured Pout of the transmitter path with 5 dBm input power is around 22 dBm compared to simulated Pout of 22.7 dBm.

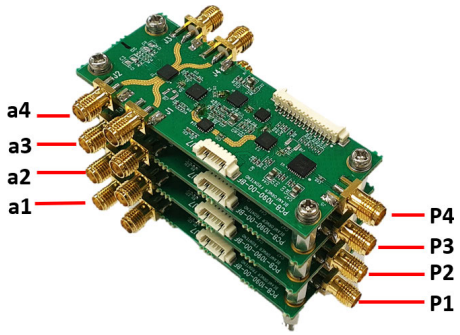

FIGURE 16. 4 T/R modules stacked-up to characterise the gain distribution.

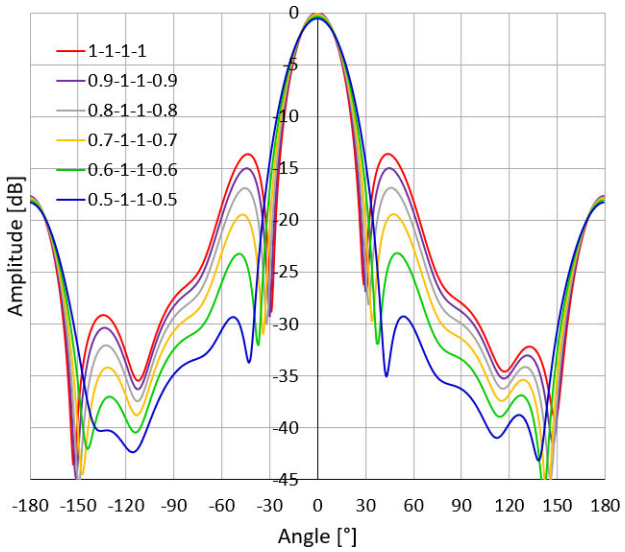

FIGURE 17. Simulated results of the SLL performance with different amplitude distribution factor.

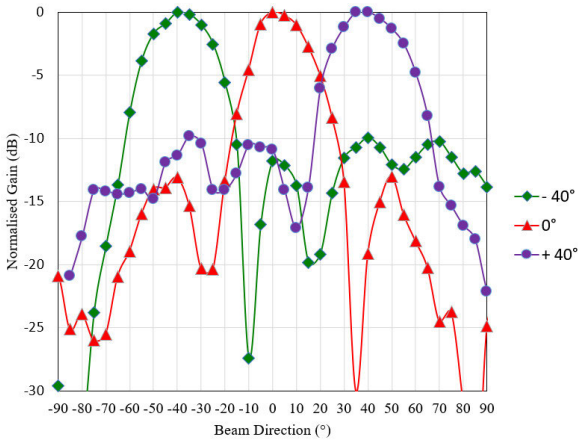

FIGURE 18. Measured beamforming result with 4 × 4 array.

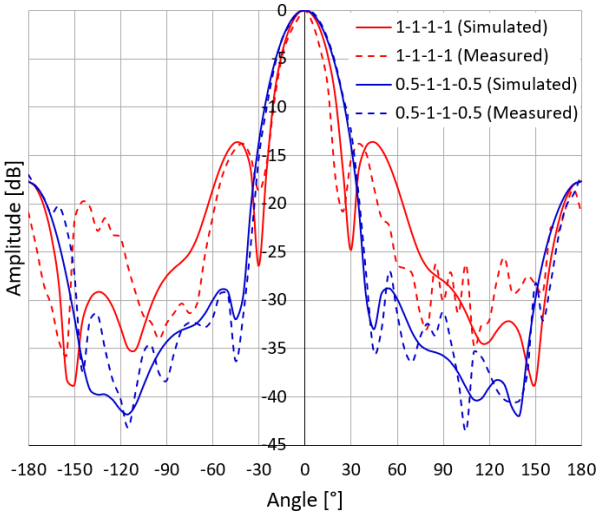

FIGURE 19. Measured results of the SLL performance with different amplitude distribution factor.

B. CHARACTERIZING THE PHASE ERROR

The frequency response, manufacturing tolerance, and components tolerance are the major contributors to the phase tolerance in the RF chain. The phase tolerance must be properly identified and compensated to provide an accurate beam steering performance of the beamforming system. The phase error was measured relative to the input phase to the T/R module, the similar phase calibration can be performed for receiver phase error correction. The phase error of the RF chain is measured using the VNA as described in Fig. 9b over the frequency band from 5180 to 5880 MHz, the phase calibration result is shown in Fig. 14. The uncalibrated phase error is shown in the blue line with 13° phase error, and the phase offset required to compensate the phase error is described by the orange line, ϕc. The red line represents the phase error after calibration with the phase error being improved to $+/-1°$.

C. CHARACTERIZING THE AMPLITUDE DISTRIBUTION

The gain distribution model is presented in Fig. 15. The antenna array [22] consists of 4 vertical elements combined into a single port using the corporate fed method, in this case, 4 units of T/R modules as shown in Fig. 16. are used to evaluate the amplitude distribution of the antenna system. The notation for the amplitude distribution is presented as a1–a2–a3–a4 where a1 is the amplitude ratio for port 1, a2 is the amplitude ratio for port 2 and so on, the amplitude ratio ranged between 0 and 1 where 1 is the full power and 0.5 is half power.

The amplitude distributions of the T/R module integrated with the 4 × 4 array is simulated using Computer Simulation Technology (CST) tool [26], the simulation results at 5.5 GHz operating frequency are presented in Fig. 17. As we can observe from the results, the antenna radiation pattern is compromised between the gain, HPBW and SLL, and the optimal results are observed when the amplitude distribution factor is 0.5-1-1-0.5 (optimum distribution) where the gain is 17.4 dBi, HPBW is 29.2° and SLL is −28.7 dB compared to the uniform amplitude distribution of 1-1-1-1 that produces the gain of 17.9 dBi, HPBW of 24.5° and SLL of −13.6 dB, thus, the optimum amplitude distribution delivers good SLL improvement of 15.1 dB for interference performance and reasonable gain and HPBW as compared to uniform distributions. The SLL improvement can further

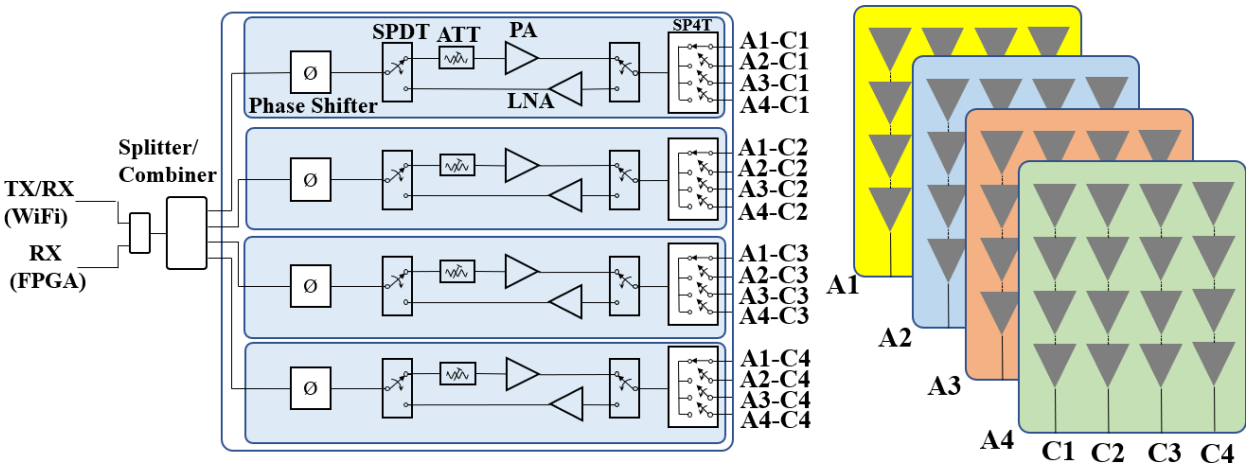

FIGURE 20. 360° beamforming system consists of 4 units of T/R modules and antenna arrays.

enhance the interference rejection in the smart antenna system. Further simulation has been carried out to evaluate the SLL improvement with amplitude distribution 0.5-1-1-0.5 for the entire steering angle supported by the array, SLL of −22.71 dBm and −12.55 dBm which is 11.1 dB and 5.27 dB improvement respectively were observed for ± 20° and ±40° steering angle. However, the amplitude distribution was not able to suppress the grating lobe level at the end-fire around ± 40°.

IV. MEASURED RESULTS AND DISCUSSION

The beamforming performance of the antenna array is measured by asserting the RF signal into each port of the antenna array with different phase shift added by the phase offset c calibrated earlier. The phase difference to each port is set by controlling the bit0 to bit5 of the 6-bits phase shifter. The phase difference for each port to enable 0°, + 40° and − 40° beam steering are presented in TABLE 2. below, where ϕc_1, ϕc_2, ϕc_3, and ϕc_4 denote the calibrated offset value for each port.

TABLE 2. Phase compensation for beamforming chains.

	- 40°	0°	+ 40°
Chain 1 (°)	ϕ_{c1}	ϕ_{c1}	45 + ϕ_{c1}
Chain 2 (°)	135 + ϕ_{c2}	ϕ_{c2}	270 + ϕ_{c2}
Chain 3 (°)	270 + ϕ_{c3}	ϕ_{c3}	135 + ϕ_{c3}
Chain 4 (°)	45 + ϕ_{c4}	ϕ_{c4}	ϕ_{c4}

The beamforming results evaluated with the compensated phase and chain power are presented in Fig. 18, where the beam steering angle agreed well with the simulated results. The compensated phase ϕ_c has successfully offset the phase difference between the RF chains. It was observed that the achievable beam-steering resolution angle is around 2° by using the 6-bits phase shifter at each RF chain.

The SLL performance results at 5.5 GHz for 0° beam with amplitude distribution of 1-1-1-1 and 0.5-1-1-0.5 are experimentally validated using the T/R modules and the 4×4 linear arrays and presented in Fig. 19. The optimum sidelobe and gain are achieved when the amplitude distribution is at 0.5-1-1-0.5 where the results are agreed well with the simulation results presented earlier.

For smart antenna system that requires 360° coverage, 4 of the T/R modules will be cascaded and the RF ports will be connected to the 4 antenna arrays respectively as shown in Fig. 20. for example, the port A1.C1 of the T/R module is connected to array A1 port C1, port A2.C1 is connected to array A2 port C1 and so on. Similar beam steering performance is expected for the rest of the other 3 sectors that makes 360° coverage of the smart antenna.

TABLE 3. T/R module comparison.

Items	[12]	[13]	[15]	This work
Frequencies	8 – 12 GHz	9 – 10 GHz	40 – 45 GHz	4.9 – 5.9 GHz
Phase Shifter / resolution	6-bit / 5.625°	LO Sync.	4-bit / 22.5°	6-bit / 5.625°
SLL	NA	-7.6 dB (+/- 20°)	~ -13 dB (± 45°) Figure 3.	-28.7 dB (0°) -22.71 dB (± 20°) -12.77 dB (± 40°)
Phase Error	5.463°	2.1°	< 8.8°	± 1°
Amplitude Error	1.25 dB	NA	< 1.3 dB	± 0.2 dB

Note: NA denotes information not available.

TABLE 3. tabulated the performance comparison with the state-of-the-art T/R modules, the proposed T/R module has the comparable or better performance compared to the state-of-the-art modules, the proposed recursive calibration process has managed to correct the phase error to ± 1° and amplitude error to ± 0.2 dB. In addition, the amplitude distribution of 0.5-1-1-0.5 combination has successfully suppressed the SLL to -28.7 dB for 0° beam, −22.71 dB for ± 20° beam and −12.77 dB for ± 40°. The recursive calibration method has improved the SLL and phase error of the antenna system without the need to alter the geometry of the antenna design which is time consuming and costly.

The proposed T/R module is also contributed to the overall cost reduction due to the utilization of COTS components and volume production. The material cost for the T/R module is around U$193.7 for sample build and the cost drop significantly to U$85.3 for mass production volume of 2,500 pcs. Another cost benefit for mass volume production is the manufacturing setup cost, which constitutes to U$200 for sample production and drops to U$1 for volume production. The cost is around 5 to 10 times lower than other commercial T/R module. Due to the low-cost structure by utilizing the COTS components, there is limited room for re-configuring the T/R module into other specification such as different operating frequency. However, with the modular concept, simple design approach and adaptation of COTS components make it easy to reproduce such T/R module in other operating specification.

V. CONCLUSION AND FUTURE WORKS

In this work, a beamforming T/R module for linear phased array application in the commercial frequency band 4.9–5.9 GHz ISM band has been developed and demonstrated. The design consideration of the T/R module including circuits design, schematic, PCB, and interface controller boards has been discussed in detail. The performance of the T/R module has been calibrated and characterized using a simple recursive calibration approach, and the beamforming performance has been experimentally evaluated using the 4×4 phased array. Leverage on the commercially available RF components and low-cost high volume manufacturing technology, the adoption of the T/R module is expected to accelerate the smart antenna deployment in the commercial infrastructure such as the 4.9–5.9 GHz ISM band which is widely used as free access such as the wireless hotspot in commercial building and public areas. For future works, based on the design concepts of the T/R module that adopts the commercially off-the-shelf RF components and standard manufacturing technology, the T/R module can be easily developed into other un-licensed bands such as 2.4 GHz, 24 GHz and 60 GHz which are commercially available for public use. In addition, the T/R module can be further miniaturized for better cost performance.

ACKNOWLEDGMENT

The authors would like to thank the Singapore Economic Development Board (EDB) and RFNet Technologies Pte Ltd., for financing and providing a good environment and facilities to support the project.

REFERENCES

[1] S. Han, C.-L. I, Z. Xu, and C. Rowell, "Large-scale antenna systems with hybrid analog and digital beamforming for millimeter wave 5G," *IEEE Commun. Mag.*, vol. 53, no. 1, pp. 186–194, Jan. 2015.

[2] L. Yang, Y. Zeng, and R. Zhang, "Wireless power transfer with hybrid beamforming: How many RF chains do we need?" *IEEE Trans. Wireless Commun.*, vol. 17, no. 10, pp. 6972–6984, Oct. 2018.

[3] S. Ahmed, M. Sadek, A. Zekry, and H. Elhennawy, "Hybrid analog and digital beamforming for space-constrained and energy-efficient massive MIMO wireless systems," in *Proc. 40th Int. Conf. Telecommun. Signal Process. (TSP)*, Barcelona, Spain, Jul. 2017, pp. 186–189.

[4] J. S. Herd and M. D. Conway, "The evolution to modern phased array architectures," *Proc. IEEE*, vol. 104, no. 3, pp. 519–529, Mar. 2016.

[5] M. Oppermann and R. Rieger, "RF modules (Tx-Rx) with multifunctional MMICs," in *Proc. IMAPS Nordic Conf. Microelectron. Packag. (NordPac)*, Gothenburg, Sweden, Jun. 2017, pp. 57–60.

[6] B. Epstein, R. H. Olsson, and K. Bunch, "Arrays at commercial timescales: Addressing development and upgrade costs of phased arrays," in *Proc. IEEE Radar Conf. (RadarConf)*, Oklahoma City, OK, USA, Apr. 2018, pp. 327–332.

[7] W. Wojtasiak, D. Gryglewski, T. Morawski, and E. Sedek, "Designing T/R module for active phased array radar," in *Proc. 14th Int. Conf. Microw., Radar Wireless Commun. (MIKON)*, Gdansk, Poland, vol. 2, May 2002, pp. 631–634.

[8] G. M. Rebeiz, K. Jin Koh, T. Yu, D. Kang, C. Young Kim, Y. Atesal, B. Cetinoneri, S. Young Kim, and D. Shin, "Highly dense microwave and millimeter-wave phased array T/R modules and butler matrices using CMOS and SiGe RFICs," in *Proc. IEEE Int. Symp. Phased Array Syst. Technol.*, Waltham, MA, USA, Oct. 2010, pp. 245–249.

[9] T. Boles, D. J. Carlson, and C. Weigand, "MMIC based phased array radar T/R modules," in *Proc. IEEE Int. Conf. Microw., Commun., Antennas Electron. Syst. (COMCAS)*, Tel Aviv, Israel, Nov. 2011, pp. 1–4.

[10] D. Conway, M. Fosberry, G. Brigham, E. Loew, and C. Liu, "On the development of a C-band active array front-end for an airborne polarimetric radar," in *Proc. IEEE Int. Symp. Phased Array Syst. Technol.*, Waltham, MA, USA, Oct. 2013, pp. 198–201.

[11] A. Fina, A. Di Carlofelice, and F. De Paulis, "High power, thermally efficient, X-band 3D T/R module with calibration capability for space radar," *IEEE Access*, vol. 6, pp. 60921–60929, Oct. 2018.

[12] Z. Wang, J. Xiao, J. Huang, H. Yin, Y. Yang, B. Yan, and B. Zhao, "An improved high-power X-band 4×4 tile-type LTCC T/R module based on liquid cooling micro-channels," in *IEEE MTT-S Int. Microw. Symp. Dig.*, Boston, MA, USA, Jun. 2019, pp. 1042–1045.

[13] Y. M. Wu, C.-Y. Ke, C. C. Wang, Y. H. Tang, Y.-W. Chen, C.-T. Li, L.-H. Chang, C.-Y. Chu, B. Su, T.-S. Chu, and Y.-J. Wang, "An X-band scalable 4×4 digital phased array module using RF SoC and antenna-in-package," in *Proc. IEEE Radar Conf. (RadarConf)*, Boston, MA, USA, Apr. 2019, pp. 1–6.

[14] H. B. Zhang, Z. L. Zhou, S. T. Yu, and D. M. Li, "Integrated antenna-TR module design for millimeter band phased-array," in *Proc. Int. Conf. Microw. Millim. Wave Technol. (ICMMT)*, Chengdu, China, May 2018, pp. 1–3.

[15] K. Koh, J. W. May, and G. M. Rebeiz, "A millimeter-wave (40–45 GHz) 16-element phased-array transmitter in 0.18-μm SiGe BiCMOS technology," *IEEE J. Solid-State Circuits*, vol. 44, no. 5, pp. 1498–1509, May 2009.

[16] H. M. M. Makkawi, "Comparative study of the radiation characteristics between uniform, Tschebyscheff and binomial amplitude distributions of linear patch antenna array for X-band radar warning receivers," in *Proc. Int. Conf. Commun., Control, Comput. Electron. Eng. (ICCCCEE)*, Khartoum, Sudan, Jan. 2017, pp. 1–8.

[17] A. P. Joubko, N. M. Naumovich, and O. A. Yurtsev, "Influence of amplitude distribution within a module and over a system of modules on the pattern of multimodule antenna array," in *Proc. Int. Conf. Antenna Theory Techn. (ICATT)*, Kharkiv, Ukraine, Apr. 2015, pp. 1–3.

[18] D. Vollbracht and G. Michalek, "X-band phase- and amplitude distribution network for phased array antenna measurements," in *Proc. 10th Eur. Conf. Antennas Propag. (EuCAP)*, Davos, Switzerland, Apr. 2016, pp. 1–5.

[19] T. Haynes, "Primer on digital beamforming," in *Spectrum Signal Processing*. 1998. Accessed: Jul. 15, 2020. [Online]. Available: http://spectrumsignal.com/resources/pdf/articles/Primer_on_Digital_Beamforming.pdf

[20] N. Nakamoto, T. Takahashi, Y. Konishi, and I. Chiba, "Phase optimization for accurate beam forming of phased array with element field errors at every phase shift," in *Proc. IEEE Int. Symp. Phased Array Syst. Technol.*, Waltham, MA, USA, Oct. 2013, pp. 693–697.

[21] Q. Fei, Y. Yu, X. Yin, L. Yang, and Y. Lu, "Low-cost phase shifter and calibration solution for multi-channel receiver," in *Proc. IEEE Int. Conf. Ubiquitous Wireless Broadband (ICUWB)*, Nanjing, China, Oct. 2016, pp. 1–3.

[22] M. C. Tan, M. Li, Q. H. Abbasi, and M. A. Imran, "A wideband beamforming antenna array for 802.11ac and 4.9 GHz in modern transportation market," *IEEE Trans. Veh. Technol.*, vol. 69, no. 3, pp. 2659–2670, Mar. 2020.

[23] C. A. Balanis, "Smart antennas," in *Antenna Theory: Analysis and Design*, 4th ed. Hoboken, NJ, USA: Wiley, 2016, ch. 16, sec. 16.8, pp. 946–959.
[24] M. C. Tan, M. Li, Q. H. Abbasi, and M. Imran, "A flexible low-cost hybrid beamforming structure for practical beamforming applications," in *Proc. IEEE Int. Symp. Radio-Frequency Integr. Technol. (RFIT)*, Nanjing, China, Aug. 2019, pp. 1–3.
[25] Pads. (2020). *PADS PCB Design Software—Mentor Graphics*. Accessed: Feb. 25, 2020. [Online]. Available: https://psds.com
[26] 3DS. (2019). *CST Studio Suite 3D EM Simulation and Analysis Software*. Accessed: Oct. 23, 2019. [Online]. Available: https://www.3ds.com/products-services/simulia/products/cst-studio-suite/

MOH CHUAN TAN (Graduate Student Member, IEEE) received the B.Tech. degree in electronic engineering from the National University of Singapore, in 2001. He is currently pursuing the Ph.D. degree in electronic engineering with the University of Glasgow, U.K. From 1991 to 2001, he was with Kenwood Electronic Technologies (S) Pte Ltd., Singapore. He was a Land Mobile Radio Transceiver Designer, he helped to set up the Kenwood Research and Development Center in Singapore, developed and managed five models of land mobile radio product design, including the Kenwood award winning model UBZ-LF14, in 1999 (a Family Radio Service radio transceiver for USA). Since 2001, he joined RFNet Technologies Pte Ltd., Singapore, as a Pioneer Member who set up the Research and Development Department and successfully designed many wireless LAN products for industrial applications such as automotive, railway, industrial IoT, and so on. He is also the Technical Director of the Research and Development Department who oversees the product and technology development. His research interests include smart antennas and RF modular frontends and systems.

MINGHUI LI (Member, IEEE) is currently an Associate Professor of electronic systems with the University of Glasgow, based in Singapore (UGS). Before joining Glasgow University, he has been working as a Lecturer with the Centre for Ultrasonic Engineering, Department of Electronic and Electrical Engineering, University of Strathclyde, U.K. He has investigated a range of industrial, UK EPSRC, knowledge exchange, and university strategic research projects as a Principal Investigator or a Co-Investigator, through collaboration and partnership with industrial companies and Research and Development organisations, such as Rolls Royce, Shell, E.ON, Serco, and the National Nuclear Laboratory from Key Sectors of Energy, Oil and Gas, Aerospace, Nuclear, Transportation and Healthcare, U.K. His research interests include sensing systems, signal processing and imaging in both fundamental algorithm research and applied prototype system development, covering a diversity of applications in communications, radar, sonar, non-destructive evaluation (NDE), and biomedical diagnosis and imaging.

QAMMER H. ABBASI (Senior Member, IEEE) received the B.Sc. and M.Sc. degrees (Hons.) in electronics and telecommunication engineering from the University of Engineering and Technology (UET), Lahore, Lahore, Pakistan, and the Ph.D. degree in electronic and electrical engineering from the Queen Mary University of London (QMUL), U.K., in January 2012. From 2012 to June 2012, he was Postdoctoral Research Assistant with the Antenna and Electromagnetics group, QMUL. From 2012 to 2013, he was an international Young Scientist under the National Science Foundation China (NSFC), and an Assistant Professor with UET, Lahore. From August, 2013 to April 2017, he was with the Center for Remote healthcare Technology and the Wireless Research Group, Department of Electrical and Computer Engineering, Texas A&M University at Qatar (TAMUQ), initially as an Assistant Research Scientist and later was promoted to an Associate Research Scientist and a Visiting Lecturer, where he was leading multiple Qatar national research foundation grants (worth £3.5 million). He is currently a Lecturer (Assistant Professor) with the School of Engineering, University of Glasgow, a Visiting Lecturer (Assistant Professor) with QMUL, and a Visiting Associate Research Scientist with TAMUQ. He has been mentoring several undergraduate, graduate students, and postdocs. He has research portfolio of around $3 million and contributed to a patent, five books and more than 200 leading international technical journal and peer-reviewed conference papers, and received several recognitions for his research. He became an IEEE Senior Member at the age of 29. He is a member of IET and a committee member of IET Antenna & Propagation and healthcare network. He has been a member of the technical program committees of several IEEE flagship conferences and a technical reviewer for several IEEE and top notch journals. He contributed in organizing several IEEE conferences, workshop, and special sessions in addition to European school of antenna course. He was the Chair of IEEE young professional affinity group. He is an Associate Editor of IEEE Access journal and acted as a guest editor for numerous special issues in top notch journals.

MUHAMMAD ALI IMRAN (Senior Member, IEEE) received the M.Sc. (Hons.) and Ph.D. degrees from Imperial College London, U.K., in 2002 and 2007, respectively. He is currently a Professor of communication systems with the University of Glasgow, the Dean of the University of Glasgow, UESTC, the Head of the Communications Sensing and Imaging (CSI) research group, and the Director of the Centre of Educational Development and Innovation, Glasgow College, UESTC. He is also an Affiliate Professor with the University of Oklahoma, USA, and a Visiting Professor with the 5G Innovation Centre, University of Surrey, U.K., where he has worked previously, from June 2007 to August 2016. He has led a number of multimillion-funded international research projects encompassing the areas of energy efficiency, fundamental performance limits, sensor networks, and self-organising cellular networks. He also led the new physical layer work area for 5G innovation centre at Surrey. He has a global collaborative research network spanning both academia and key industrial players in the field of wireless communications. He has supervised more than 40 successful Ph.D. graduates and published over 400 peer-reviewed research articles, including more than 50 IEEE Transaction articles. He secured first rank in his B.Sc. and a distinction in his M.Sc. degree along with an award of excellence in recognition of his academic achievements conferred by the President of Pakistan. He has given an invited TEDx talk, in 2015, and more than 50 plenary talks, tutorials and seminars in International conferences, events, and other institutions. He has taught on international short courses in USA and China. He is the co-founder of IEEE Workshop BackNets 2015 and chaired several tracks/workshops of international conferences. He is a Fellow of IET and a Senior Fellow of Higher Education Academy (SFHEA), U.K. He has been awarded the IEEE Comsoc's Fred Ellersick Award, in 2014, the TAO's Best Paper Award in IEEE ICC, in 2019, the FEPS Learning and Teaching Award, in 2014, the Sentinel of Science Award, in 2016, and twice nominated for Tony Jean's Inspirational Teaching Award. He has won more than seven best paper awards in international conferences. He is a shortlisted finalist for The Wharton-QS Stars Awards 2014 for innovative teaching and VC's learning and teaching award in the University of Surrey. He is the UK&RI Chair for the Backhaul/Fronthaul Networking & Communications Emerging Technologies Initiatives (ETI-BNC) of IEEE ComSoc. He has been an Associate Editor of IEEE Communications Letters and *IET Communications Journal*. He is also serving as an Associate Editor for the IEEE Transactions on Communications and IEEE Access. He has served as a Guest Editor for many prestigious international journals, including the IEEE Journal on Selected Areas in Communications (JSAC).